Molecular Vision 2015; 21:811-827 <http://www.molvis.org/molvis/v21/811>
Received 11 November 2014 | Accepted 29 July 2015 | Published 31 July 2015

Variable phenotypic expressivity in inbred retinal degeneration mouse lines: A comparative study of C3H/HeOu and FVB/N *rd1* mice

Michiel van Wyk, Sabine Schneider, Sonja Kleinlogel

Department of Physiology, University of Bern, Bern, Switzerland

Purpose: Recent advances in optogenetics and gene therapy have led to promising new treatment strategies for blindness caused by retinal photoreceptor loss. Preclinical studies often rely on the *retinal degeneration 1* (*rd1* or Pde6b^{rd1}) retinitis pigmentosa (RP) mouse model. The *rd1* founder mutation is present in more than 100 actively used mouse lines. Since secondary genetic traits are well-known to modify the phenotypic progression of photoreceptor degeneration in animal models and human patients with RP, negligence of the genetic background in the *rd1* mouse model is unwarranted. Moreover, the success of various potential therapies, including optogenetic gene therapy and prosthetic implants, depends on the progress of retinal degeneration, which might differ between *rd1* mice. To examine the prospect of phenotypic expressivity in the *rd1* mouse model, we compared the progress of retinal degeneration in two common *rd1* lines, C3H/HeOu and FVB/N.

Methods: We followed retinal degeneration over 24 weeks in FVB/N, C3H/HeOu, and congenic Pde6b^{+} seeing mouse lines, using a range of experimental techniques including extracellular recordings from retinal ganglion cells, PCR quantification of cone opsin and *Pde6b* transcripts, in vivo flash electroretinogram (ERG), and behavioral optokinetic reflex (OKR) recordings.

Results: We demonstrated a substantial difference in the speed of retinal degeneration and accompanying loss of visual function between the two *rd1* lines. Photoreceptor degeneration and loss of vision were faster with an earlier onset in the FVB/N mice compared to C3H/HeOu mice, whereas the performance of the Pde6b^{+} mice did not differ significantly in any of the tests. By postnatal week 4, the FVB/N mice expressed significantly less cone opsin and Pde6b mRNA and had neither ERG nor OKR responses. At 12 weeks of age, the retinal ganglion cells of the FVB/N mice had lost all light responses. In contrast, 4-week-old C3H/HeOu mice still had ERG and OKR responses, and we still recorded light responses from C3H/HeOu retinal ganglion cells until the age of 24 weeks. These results show that genetic background plays an important role in the *rd1* mouse pathology.

Conclusions: Analogous to human RP, the mouse genetic background strongly influences the *rd1* phenotype. Thus, different *rd1* mouse lines may follow different timelines of retinal degeneration, making exact knowledge of genetic background imperative in all studies that use *rd1* models.

Retinitis pigmentosa (RP) is a heterogenic hereditary disease resulting in progressive photoreceptor loss, eventually leading to blindness. Recent advances in gene therapy and optogenetics have led to promising therapeutic strategies for patients with RP and, accordingly, to a sharp rise in the use of RP mouse models [1-3]. The genetic diversity of RP in humans, which may affect more than 100 individual genes, is reflected in the large collection of retinal degeneration (rd) mutations available in RP mouse models [4]. Most vision recovery studies, however, use the *retinal degeneration 1* (*rd1*, rodless, Pde6b^{rd1}) mouse, with a homozygous nonsense mutation in exon 7 (codon 347) of the *Pde6b* gene correlated with deficient activity of the rod cGMP-phosphodiesterase, as well as a murine leukemia provirus insertion in intron 1 of the same gene [5,6]. The popularity of the *rd1* model can be attributed to several factors: (1) It was the first identified model of RP [7], (2) its phenotype resembles that of human patients with RP with the *Pde6b* mutation, accounting for approximately 4% of all RP cases [8-10], (3) it has become a standard model, making comparisons between studies easier, and (4) it is an accessible model with a high prevalence in laboratory mice.

Currently, more than 100 mouse lines carry the *rd1* mutation, allowing experimenters to choose the genetic background according to their needs, for example, reliable breeders with large litters, pigmented or albino mice, availability at the local husbandry, and so forth. Despite the pivotal role of disease progression at the time point of therapeutic intervention and the knowledge of variable phenotypic expressivity in human RP patients [11] as well as evidence

Correspondence to: Sonja Kleinlogel, Department of Physiology, University of Bern, Bühlplatz 5, 3012 Bern, Switzerland; Phone: +41-31-631-8705; FAX: +41-31-631-4611; email: kleinlogel@pyl.unibe.ch

pointing toward variation in retinal degeneration between *rd1* mice [12], the influence of genetic background has been largely neglected in the *rd1* mouse model. Moreover, the genetic background of *rd1* mice is often omitted from regenerative studies, or strains are interchangeably referred to as Pde6b$^{-/-}$ [13-16].

In summary, the progress of retinal degeneration is considered identical in *rd1* mice: Degeneration starts with the fast onset of rod dystrophy at postnatal day (P) 8–10 [17-19]. By 3–4 weeks of age, all rod photoreceptors are lost, and a single layer of photoreceptors consisting of cones remains that are subsequently lost through secondary unknown mechanisms [17,18,20-22]. The outer segments of the cones are misshaped and presumably dysfunctional, which manifests in an undetectable electroretinogram (ERG) at P21 [23] and a total loss of image-forming vision by P40 [17]. To address the important question of potential variable phenotypic expressivity in the *rd1* mouse model, we compared the progress of photoreceptor degeneration between the two strains with the highest prevalence of *rd1* mutations, C3H and FVB [24-26]. We used the congenic C3H-Pde6b^{+} and FVB-Pde6b^{+} seeing mouse lines with matching genetic backgrounds but lacking the *rd1* mutation as the negative controls. C3H mouse lines are widely distributed for research purposes by most major animal suppliers worldwide. A review of more than 130 research articles in which the *rd1* background was stated showed that 67% of these studies used the C3H line [27]. Retinal degeneration caused by the *rd1* mutation was first characterized in the C3H/He strain [18,21,22]. In this manuscript, we use the substrain C3H/HeOuJ, a pigmented prolific general purpose strain frequently used as a model of retinal degeneration in vision research [3,28,29]. FVB mice are also popular *rd1* models; more than 50 substrains carry the *rd1* mutation [26,30-33]. In this study, we used the FVB/N substrain, which has been proved to be a near-perfect background for creating transgenic animals with pronuclear injection [34,35]. Not only do the egg cells have large hardy pronuclei that facilitate the process of pronuclear injection, but FVB/N mice are also highly prolific breeders, which allow researchers to rapidly establish transgenic lines. The ease of generating transgenic mice led to the creation of a congenic seeing counterpart, the FVB-Pde6b^{+} strain [36,37].

Since cone degeneration determines the ultimate onset of blindness, we focused primarily on the rate of cone degeneration and the accompanying loss of visual function at photopic light intensities. We followed the progress of retinal degeneration in both mouse lines from 3 to 24 weeks of age using behavioral optokinetic reflex (OKR) experiments, in vivo flash ERG recordings, recordings of light responses from retinal ganglion cells in isolated retinas, cone opsin and rod photoreceptor cGMP−specific phosphodiesterase beta−subunit (β-PDE) immunoreactivity as well as PCR quantification of cone opsin and Pde6b transcript levels. We demonstrate a marked difference in the speed of photoreceptor degeneration and the associated loss of visual function between the two *rd1* lines. Degeneration was significantly faster with an earlier onset in FVB/N compared to the C3H/HeOu mice. In contrast, no significant differences were observed between the two congenic seeing Pde6b^{+} lines in any of the tests. We conclude that, as in human patients, secondary genetic factors are imperative in the pathology of *rd1* mice.

METHODS

Animals: Experiments were performed on either sex of the C3H/HeOuJ, FVB/NCrl and congenic seeing C3Sn.BLiA-Pde6b^{+}/J (C3H-Pde6b^{+}) and FVB.129P2-Pde6b^{+}Tyr$^{c\text{-}ch}$/AntJ (FVB-Pde6b^{+}) mice. All mouse lines were obtained from Charles River Laboratories (Sulzfeld, Germany), the European distributor of the Jackson Laboratory, which maintains its own FVB/N strain (FVB/NCrl).

The C3H parent colony was developed by L. C. Strong in 1920 from a cross of a Bagg albino female with a DBA male followed by selection for high incidence of mammary tumors. The tumors resulted from exogenous mouse mammary tumor virus (MMTV) transmitted through the mother's milk. The Jackson Laboratory currently maintains four rederived C3H substrains that have been free of exogenous MMTV since 1999: (1) C3H/HeJ (Stock No. 000,659), (2) C3H/HeOuJ (Stock No. 000,635), (3) C3HeB/FeJ (Stock No. 000,658), and (4) C3H/HeSnJ (Stock No. 000,661). The C3H/HeSnJ strain was separated from the "parental" C3H/HeJ line before 1947, the C3HeB/FeJ line in 1948 (by embryo transfer to C57/BL6 surrogate mothers), and the C3H/HeOuJ line in 1952 when it was discovered that this colony of mice carried the Kit$^{w\text{-}x}$ mutation [38]. Since Kit$^{w\text{-}x}$ is a homozygous lethal mutation, the affected colony had a mixture of heterozygous and homozygous animals from which the current wild-type C3H/HeOuJ line was derived in 1982 by Dr. H.C. Outzen. All C3H substrains from the Jackson Laboratory share the same *rd1* Pde6b mutation resulting in photoreceptor degeneration as well as a mutation in the *AHR* gene resulting in xenobiotic sensitivity. Since their final separation in 1952 and close to 200 generations of breeding, we are aware of genetic divergence in these substrains. The C3H/HeJ substrain has been the most severely affected and acquired the following mutations: (1) a mutation in the *tlr4* gene conveying endotoxin resistance [39], (2) an insertion in the last intron of the

Gria4 gene decreasing protein expression and leading to high susceptibility to absence seizures [40], (3) an insertion in intron 19 of the *Pcnxl2* gene, again decreasing protein expression but mitigating the absence seizure phenotype [41], (4) an inversion covering 20% of chromosome 6, which does not appear to have a phenotype (Jax Notes, issue 491, Fall 2003), and, most importantly, (5) the Gpr179^{nob5} insertional mutation in intron 1 of the *Gpr179* gene that compromises visual function [27,42]. Over the same period, the C3HeB/FeJ line has acquired a mutation in the *Ipr1* gene that makes the line highly susceptible to tuberculosis [43] while no mutations have been reported in the C3H/HeOuJ and C3H/HeSnJ lines, which are considered genetically similar.

The FVB/N line stems from an outbred colony of Swiss mice (N:GP general purpose strain) established at the National Institutes of Health in 1935. A second colony (N:NIH) was established from the original N:GP colony in the early 1940s. In 1966, a project was started to develop two populations of N:NIH mice, one sensitive (HSFS/N) and one resistant (HSFR/N) to the histamine sensitivity factor. In the early 1970s, while being established as an inbred strain, some HSFS/N mice were discovered to be sensitive to the Friend leukemia virus B strain. At this point, inbreeding continued with selection for Fv-1^{b} homozygosity, and the strain was designated as FVB as an abbreviation for Friend virus B-type susceptibility. The FVB line was maintained as an inbred line without further selection and was brought to Charles River from the NIH in 1994 where the line has been maintained since. There exist no known genetic differences between the FVB/NCrl line from Charles River and the FVB/NJ line from the Jackson laboratory. In addition to the *rd1* Pde6b mutation and the Fv-1^{b} allele, all FVB lines carry three additional mutations: (1) A frame shift in the *Disc1* gene results in abnormal learning/conditioning [44], (2) a deletion and premature stop codon in the *C5* gene is associated with immune deficits and allergen-induced bronchial hypersensitivity [45], and (3) a nt7778 G/T point mutation in the mitochondrial *mt-ATP8* gene [46] is correlated with anxiety-related behavior and increased oxidative stress [47,48].

The seeing congenic mouse lines C3A.BLiA-Pde6b^{+}/J and FVB.129P2-Pde6b^{+} Tyr$^{c\text{-}ch}$/AntJ were generated at the Jackson Laboratory specifically to produce control sighted strains on C3H/He and FVB/N backgrounds [49]. C3A.BLiA-Pde6b^{+}/J was generated by introducing the C57BL/LiA-derived wild-type allele of *Pde6b* to the C3H/HeSnJ strain before offspring were backcrossed for another ten generations to the C3H/HeSnJ inbred mice. Due to the genetic identity of the C3H/HeOuJ and C3H/HeSnJ mouse lines, the C3A.BLiA-Pde6b^{+}/J makes a well-suited congenic sighted strain for the C3H/HeOuJ *rd1* mice. For generation of the sighted FVB.129P2-Pde6b^{+} Tyr$^{c\text{-}ch}$/AntJ line, the 129P2/OlaHsd-derived wild-type allele of *Pde6b* was introduced to the FVB/N background and subsequently backcrossed for 11 generations with FVB/N mice. The first homozygous matings for both strains were performed in 2006.

All animal experiments were conducted in accordance with the Swiss Federal Animal Protection Act and the standards set forth in the ARVO Statement for the Use of Animals in Ophthalmic and Visual Research and were approved by the animal research committee of Bern (approval No BE44–12). Mice were housed under a 12 h:12 h light-dark cycle with a daily light intensity of about 7 lux, which is considered non-harmful to the sensitive retinas of albino mice [50]. Light intensity was measured inside the cage, using a light meter (Model PM200, Thorlabs, Munich, Germany). Mice were euthanized with CO_2 anesthesia followed by decapitation.

Recordings from retinal ganglion cells: The methods for recording cell-attached light responses from retinal ganglion cells have been described in detail previously [12]. Mice were dark adapted for 1 h, and, following euthanasia, the eyes were enucleated under dim-red illumination and the retinas removed. The retina was placed in a recording chamber perfused with Ames medium (Sigma-Aldrich, Buchs, Switzerland) at a rate of 5 ml/min, and the tissue was maintained at 34–36 °C (pH 7.4). The ganglion cells were targeted for recording under visual control using infrared differential-interference-contrast (IR-DIC) optics. Electrodes were pulled from borosilicate glass to a final resistance of 5–8 MΩ and filled with Ames medium. Cells were approached with the recoding pipette until spontaneous action potentials were observed in the voltage recording. Blue light (λ=470 nm) flash stimuli were generated with a pE-2 system (CoolLED, Andover, UK) and projected through a 40X water immersion objective onto the receptive field of the recorded ganglion cell. The background light intensity was kept near zero. The stimulus light intensity was set to 3.2×10^{17} photons cm^{-2} s^{-1}. The stimulus was presented 5 times to evaluate whether the action potentials were modulated consistently. Spike-time histograms with 100 ms bins were generated from all five traces. Cells were classed as light responsive if there was a significant change in firing frequency between at least two bins generated before and after the onset of the light stimulus.

Optokinetic reflex measurements: The OptoMotry system from CerebralMechanics (Lethbridge, Canada) was used to measure the OKR with the method described previously [51,52]. A virtual cylinder comprising a vertical sine wave grating was projected in three-dimensional (3D) coordinate space on four computer monitors (Dell 1703FP, Bern,

Switzerland) facing a 13-cm-high platform above a mirrored floor under a likewise mirrored lid. The light intensity measured at the center of the platform was 5.6×10^{13} photons cm^{-2} s^{-1}. During testing, the mice stood unrestrained on the platform tracking the 3D pattern with a reflexive head movement that was recorded with a video camera (DCR-HC26, Sony, Bern, Switzerland). The movements of the mice on the platform were followed by two independent experimenters. The spatial frequency of the test grating was changed in steps until the highest spatial tracking frequency was identified as the threshold (visual acuity). A minimum spatial acuity of 0.003 cycles per degree was assigned to all mice with no detectable OKR reflex.

Electroretinography: All procedures were performed under dim-red illumination. We anesthetized the mice with an intraperitoneal injection of 100 mg/kg ketamine and 10 mg/kg xylazine and dilated the pupils of both eyes using a drop of 10 mg/ml atropine sulfate (Théa Pharma, Clermont-Ferrand, France). Animals were subsequently placed on a temperature-controlled heating table inside a Q400 full-field bowl (Roland Consult, Brandenburg, Germany). We recorded from both eyes using gold wire electrodes wetted with 1% methylcellulose that circled the corneal borders (OmniVision, Puchheim, Germany). Needle electrodes placed under the skin of the cheeks were used as reference electrodes while a third needle electrode positioned in the base of the tail served as a ground electrode. Responses to strobe flashes were amplified, averaged, and stored using a RetiScan-RetiPort electrophysiology unit (Roland Consult).

Immunocytochemistry: Whole mount retinas were incubated for 1 h in a blocking solution containing 2% donkey serum and 1% Triton X-100 in PBS (1X; 137 mM NaCl, 2.7 mM KCl, 10 mM Na_2PO_4, 1.8 mM KH_2PO_4, pH 7.4). Retinas were then incubated for 5 days at 4 °C in blocking solution containing 1:500 primary goat anti-OPN1 SW antibody (Santa Cruz, Santa Cruz, CA, sc-14365), followed by a 1-h washing step and overnight incubation at 4 °C in blocking solution containing 1:400 donkey anti-goat-Cy3 secondary antibody (Millipore, AP180C, Schwalbach, Germany). Photomicrographs of opsin-stained retinas were taken from the midperipheral retinal where the cone density was highest using either on a Nikon Eclipse epifluorescence microscope (Nikon, Amsterdam, Netherlands) or on a LSM5 (Carl Zeiss, Jena, Germany) laser scanning microscope. Image contrast was manipulated using ImageJ [53].

Genotyping: To extract genomic DNA for PCR, toe clippings were lysed overnight in a buffer containing 10 mM Tris, 100 mM NaCl, 10 mM EDTA, 0.5% sodium dodecyl sulfate (SDS), and 0.75 µg/ml Proteinase K (pH 8.0). The lysate was purified using silica spin columns (Macherey-Nagel, Oensingen Switzerland). Genotyping for the murine leukemia viral insertion was done using the standard 3-primer protocol [54]. Three hundred base pairs flanking the position of the nonsense mutation in codon 347 were amplified using Pittler and Baehr's protocol [6]. This PCR product was purified and sequenced at MycroSynth AG (Balgach, Switzerland) and additionally digested with DdeI, since the *rd1* allele contains an additional DdeI restriction site not present in the wild-type allele [6].

Quantitative reverse-transcription PCR: We extracted total RNA from mouse retinas using the SV Total RNA Isolation Kit (Promega, Dübendorf, Switzerland) and ran one-step quantitative reverse-transcription PCR (qPCR) reactions (40 cycles) with 20 ng total RNA using the KAPA SYBR FAST One-Step Universal Kit (Kapa Biosystems, London, UK) on an Eco Real-Time PCR System (Illumina Inc., San Diego, CA). Values obtained for Opn1sw (S-opsin) mRNA (F 5′-CTG CTA GCA GCA AAC ACA ACG-3′, R 5′-GCT ACA GGC AGA GAG TAA CAG-3) and Pde6b mRNA levels (primers spanning exon 7, F 5′-GGC CGG GAA ATT GTC TTC TAC-3′ containing exon 5 and 6 sequences, R 5′-CCC CAG GAA CTG TGT CAG AGA-3′ containing exon 9 and 10 sequences [55]) were normalized against β-Actin-mRNA levels (F 5′-CGG CAT CGT CAC CAA CTG-3′, R 5′-AAC ATG ATC TGG GTC ATC TTC TC-3′). For comparison of S-opsin expression, the Opn1sw mRNA level in the wild-type C57/BL6 mice was set to 1, and the values obtained from the C3H/HeOu and FVB/N retinas were illustrated as a fraction of the wild-type value. To compare *Pde6b* mRNA levels, the level of Pde6b expression in C3H-Pde6b$^+$ mice was set to 1.

β-PDE western blotting: Two to three mice were sacrificed, the retinas removed, and protein extracted with 30 min incubation in cell lysis buffer supplemented with a protease inhibitor cocktail (Roche). After centrifugation for 10 min at 1,000 ×g at 4 °C, the protein content of the supernatant was determined with a BCA Kit (Thermo Scientific). Aliquots containing 20 µg of protein were denatured by incubation in Laemmli buffer (Sigma) for 5 min at 100 °C and subjected to SDS–polyacrylamide gel electrophoresis (PAGE) using a 4–20% gradient gel BioRad, Cressier, Swizterland). Proteins were transferred onto a 0.2 µm polyvinylidene fluoride (PVDF) membrane (Biorad) and blocked in 5% non-fat dried milk. The blots were incubated overnight at 4 °C with anti-β−PDE polyclonal antibody (Antibodies online, ABIN122848, 1:2,000) against the N-terminal amino acid residues 20–36 from the mouse β−PDE protein and anti-GAPDH monoclonal antibody (Fitzgerald, Newmarket, UK, 10R-G1099 1:100,000) followed by incubation in horseradish peroxidase

(HRP)-conjugated secondary anti-rabbit or anti-mouse (1:1,000, Jackson Immuno Research Europe Ltd, Suffolk, UK) antibodies for 1 h at room temperature. Finally, the blots were developed with SuperSignal West Dura Extended Substrate (Thermo Scientific, 34,075) for detection of HRP enzymatic activity. The apparent molecular weights of the probed proteins were estimated from the position of the Precision Plus standard markers (BioRad, 161–0374).

Statistical analysis: Statistics were performed in Microsoft Excel or NCSS statistics software. All analyzed data sets had normal distributions (verified using the Kolmogorov–Smirnov test). Differences between the *rd1* and Pde6b$^+$ mouse lines were analyzed using an unpaired one-tailed Student *t*-test not assuming equal variance, and differences between the C3H/HeOu and FVB/N *rd1* or Pde6b$^+$ lines were analyzed with an unpaired, two-tailed Student *t*- test assuming equal variance. In the figures, significance of $p<0.05$ is indicated by an asterisk. Average values are indicated ± standard error, unless otherwise indicated. Fit functions and R-square values are indicated in the figure legends.

RESULTS

We observed more remaining photoreceptor nuclei in the retinal sections of the young, 3-week-old C3H/HeOu mice compared to the FVB/N mice (Figure 1A,B). Although the FVB/N retinas contained only one remaining row of photoreceptors, in line with previous reports for *rd1* mice [18,56], the outer nuclear layer (ONL) of the retinas from the 3-week-old C3H/HeOu mice was still approximately two to three rows thick. At 23 weeks of age, the ONL in both strains was only one cell layer thick (Figure 1C,D). We also observed differences in the morphologies of the cone outer segments (OS). The OS in retinas from the 3-week-old FVB/N mice were deformed and mostly spherical (Figure 1B,F), while they were more ordered and cylindrical in the young C3H/HeOu retinas (Figure 1A,E). At 23 weeks, all OS were lost in the FVB/N retinas with only a few misshaped, spherical OS remaining in the C3H/HeOu mice (Figure 1G,H). The loss of cone OS coincided with the accumulation of opsin in the cell bodies.

To confirm that both mouse lines carried the same *rd1* Pde6b allele, we performed PCR to probe for the presence of the Tyr347 point mutation and the provirus XMV28 insertion in intron 1 of the *Pde6b* gene. As apparent from the results depicted in Figure 2, the C3H/HeOu and FVB/N strains were *rd1* with identical mutations in *Pde6b*.

To compare the morphological and functional degeneration over time in the two strains in more detail, we performed immunocytochemistry, ERG, and electrophysiological recordings as well as in vivo OKR experiments in parallel in the FVB/N and C3H/HeOu mice at 4 week intervals from 4 to 24 weeks of age. We used seeing FVB-Pde6b$^+$ and C3H-Pde6b$^+$ mice restricted to a single age group of 7–8 weeks as controls, since the likelihood of an age-related effect in these two strains was considered low.

Quantification of Pde6b mRNA and β-PDE expression: To examine if degeneration in FVB/N mice starts earlier than in C3H/HeOu mice, we performed reverse transcription qPCR quantification of Pde6b transcripts in retinal homogenates of young, 3-week-old *rd1* mice. β-PDE is expressed only in rod photoreceptors and therefore is used as an indicator of remnant rods [57]. Pde6b mRNA transcripts were still detectable in both *rd1* lines (compared to C57/BL6: FVB/N 1.0±0.5%, n=7; C3H/HeOu 11.6±2.1%, n=8), indicating that some rod photoreceptors still remained but at significantly lower numbers compared to the congenic Pde6b$^+$ control mice (C3H-Pde6b$^+$ 89±11%, FVB-Pde6b$^+$ 100±24%, n=8; Figure 3A,B). More importantly, the Pde6b transcript levels in the FVB/N retinas were significantly reduced compared to those in the C3H/HeOu retinas, corroborating the relatively progressed rod degeneration shown in Figure 1B. Since a gene's mRNA level does not predict protein levels, we also performed high-sensitivity chemiluminescent western blotting for β-PDE. The retinal protein extracts from the *rd1*, Pde6b$^+$, and C57/BL6 mice (used as a positive internal control) were probed with an N-terminal anti-β-PDE antibody (AA residues 20–36). β-PDE immunoreactivity to the full-length protein of approximately 86 kDa was visualized to similar amounts in extracts from the Pde6b$^+$ and C57/BL6 retinas (Figure 3C). In contrast and in line with previous reports [56], no such immunoreactivity was detected in either *rd1* line (FVB/N or C3H/HeOu), to neither full-length nor truncated 38 kDa β-PDE protein, even when the blots were extensively overdeveloped (Figure 3C).

Immunocytochemistry and qPCR quantification of opsin expression: As degeneration of the cone OS ultimately determines the onset of blindness [58], we performed anti-S-opsin immunostaining on retinal whole mounts (Figure 4) at 4-week age intervals and in all four mouse lines. We chose S-opsin (*Opn1sw*), which is also expressed by most green cones [59], for immunocytochemistry to allow comparison with previous work in *rd1* mice. In the 3- to 4-week-old C3H/HeOu mice, and more apparent in the 3- to 4-week-old FVB/N mice, the cone OS were relatively small and misshaped or lobular compared to those of the healthy FVB-Pde6b$^+$ and C3H-Pde6b$^+$ retinas (Figures 1 and 4). This is in good agreement with the literature, which states that photoreceptor outer and inner segments are never fully developed in *rd1* mice [17,60]. We performed OS counts in the

mid-peripheral retinas of 4-week-old *rd1* mice, where cone density is the highest, and found similar numbers for C3H/HeOu (8.43±0.9 k/mm^2, n=6) and FVB/N (7.08±0.54 k/mm^2, n=6) mice that did not significantly differ from the counts of their seeing congenics (C3H-Pde6b$^+$ (9.45±0.75 k/mm^2, n=5; FVB-Pde6b$^+$ 8.72±0.68 k/mm^2, n=5). In both *rd1* lines, the OS count decreased with age resulting in a synchronous rise in the number of labeled cone cell bodies (Figure 4). The latter is most likely a direct consequence of OS loss, where opsin naturally destined for the OS now accumulates in the soma. As described previously, cone cell bodies labeled with opsin staining form dendrite-like processes without any OS [13]. OS degeneration progressed at different speeds in the FVB/N and C3H/HeOu mice. Although the OS had virtually disappeared by 16 weeks of age in the FVB/N mice (0.77±0.77 k/mm^2), they were lost only by week 24 in the C3H/HeOu mice (0.81±0.33 k/mm^2).

As an additional measure of cone degeneration, we quantified S-opsin expression in retinal homogenates. For the C3H/HeOu mice, the qPCR data supported the morphological findings in that the number of S-opsin transcripts was similar to those from the two seeing C3H-Pde6b$^+$ and FVB-Pde6b$^+$ strains. However, the S-opsin transcripts were already significantly reduced in the 4-week-old FVB/N retinas (Figure 3D). The reduced S-opsin transcript levels despite the relatively

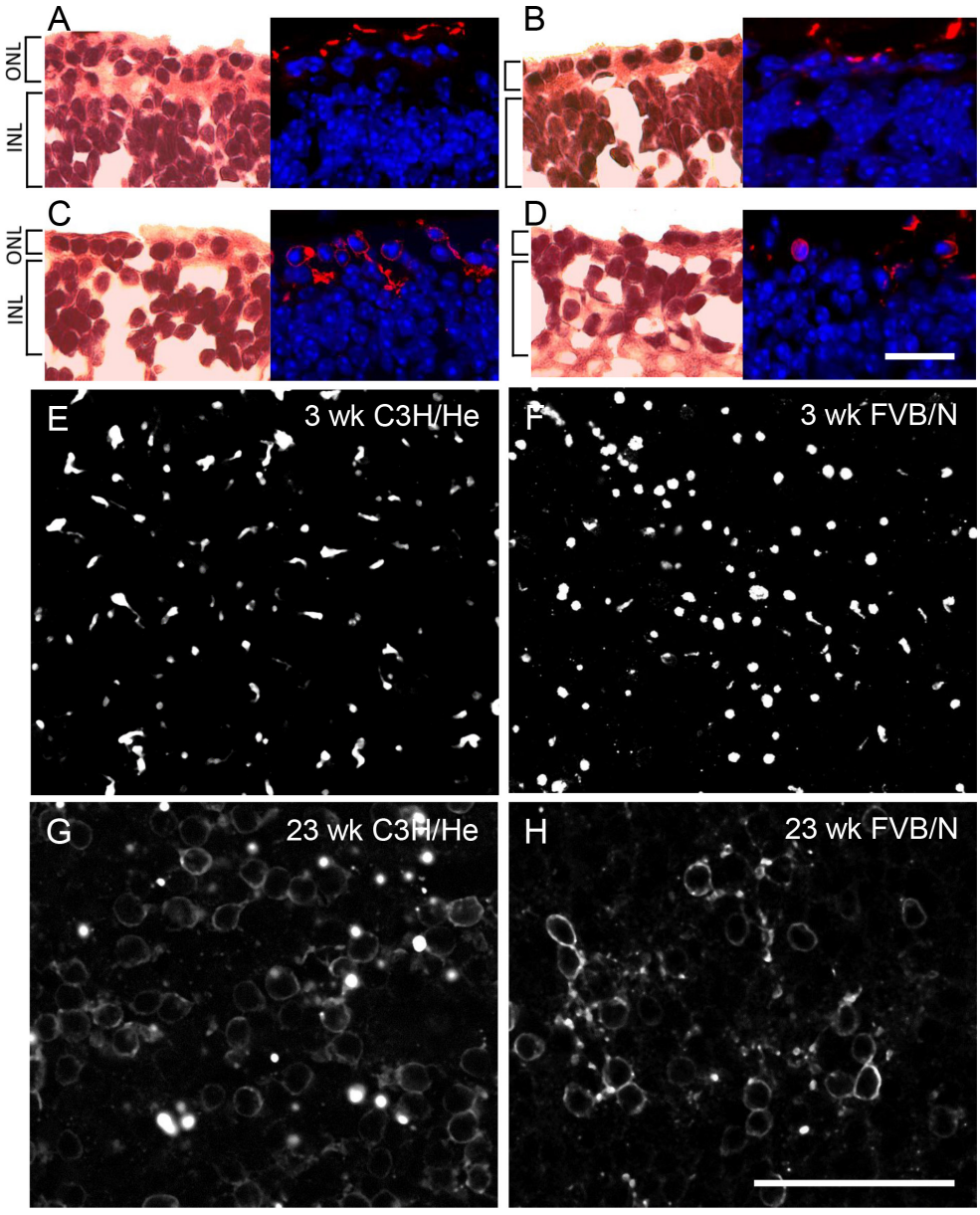

Figure 1. Comparison of retinal morphologies of 3-week-old and 23-week-old FVB/N and C3H/HeOu mice. **A–D**: Longitudinal retinal cryosections stained with hematoxylin and eosin (left panels) and against S-opsin and 4',6-diamidino-2-phenylindole (DAPI) (right panels). **E–H**: Retinal whole mounts stained against S-opsin. The outer nuclear layer (ONL) is two to three cell layers thick in 3-week-old C3H/HeOu mice (**A**), whereas the ONL of the FVB/N mice had only one layer of remnant photoreceptors (**B**). In 23-week mice of both lines, the ONL was one cell layer thick (**C**,**D**). At 3 weeks of age, the OS are more ordered and cylindrical in the C3H/HeOu retinas (**A**,**E**) compared to the FVB/N retinas (**B**,**F**). At 23 weeks (**G**,**H**), the OS are lost, and S-opsin is located in the cell bodies. Note that the FVB/N retina contains markedly fewer cones. Scale bars, (**A–D**) 20 µm, (**E–H**) 50 µm.

high OS count in 4-week-old FVB/N mice may indicate more advanced pathological progress in the relatively misshaped FVB/N compared to the C3H/HeOu cones.

Light responses recorded from retinal ganglion cells: To investigate if the morphological discrepancies manifest functionally, we recorded extracellular light responses from retinal ganglion cells in isolated retinas (Figure 5). In both Pde6b$^+$ mouse lines, approximately 90% of all cells responded to a step change in light intensity centered over the receptive field, 90±5% for C3H-Pde6b$^+$ and 93±4% for FVB-Pde6b$^+$. The small fraction of cells that did not respond to the light stimulus in the Pde6b$^+$ mice may be cells with highly selective trigger features not activated by the flashing spot stimulus [61]. In the 4-week-old C3H/HeOu *rd1* mice, 84±11% of the ganglion cells responded to the light stimulus, not significantly less than in Pde6b+ retinas. At 8 weeks, 67±13% of the C3H/HeOu ganglion cells still responded. The number of responding cells decreased steadily with age, with an eventual loss of light response at the age of 24 weeks (2±3%; Figure 5), coinciding with OS loss (Figure 4D). Characteristic slow light responses recorded from melanopsin-containing ganglion cells persisted but were not included in the analysis [62]. In contrast and in line with our morphological observations, significantly fewer ganglion cells responded in 4-week-old FVB/N mice (46±12%), and their number declined further to 23±8% at 8 weeks, with a complete lack of retinal responsiveness by postnatal week 12.

ERG experiments: We performed photopic ERG measurements to confirm the electrophysiological data. Again, the seeing FVB-Pde6b$^+$ and C3H-Pde6b$^+$ mice had strong photopic ERG responses to a 100 cd/m^2 Xenon strobe flash, with average b-wave amplitudes of 178±17 µV and 190±20 µV, respectively (Figure 6). In contrast to the patch-clamp experiments, the ERG responses from the 4-week-old C3H/HeOu mice were much weaker compared to the seeing congenic mice with a significantly reduced b-wave (22±14 µV). Nevertheless, it is remarkable that an ERG was still present in the C3H/HeOu mice, since the literature reports loss of an ERG in *rd1* mice by P21 [18,23]. In line with the literature, no ERG was detected at any time point in the FVB/N mice.

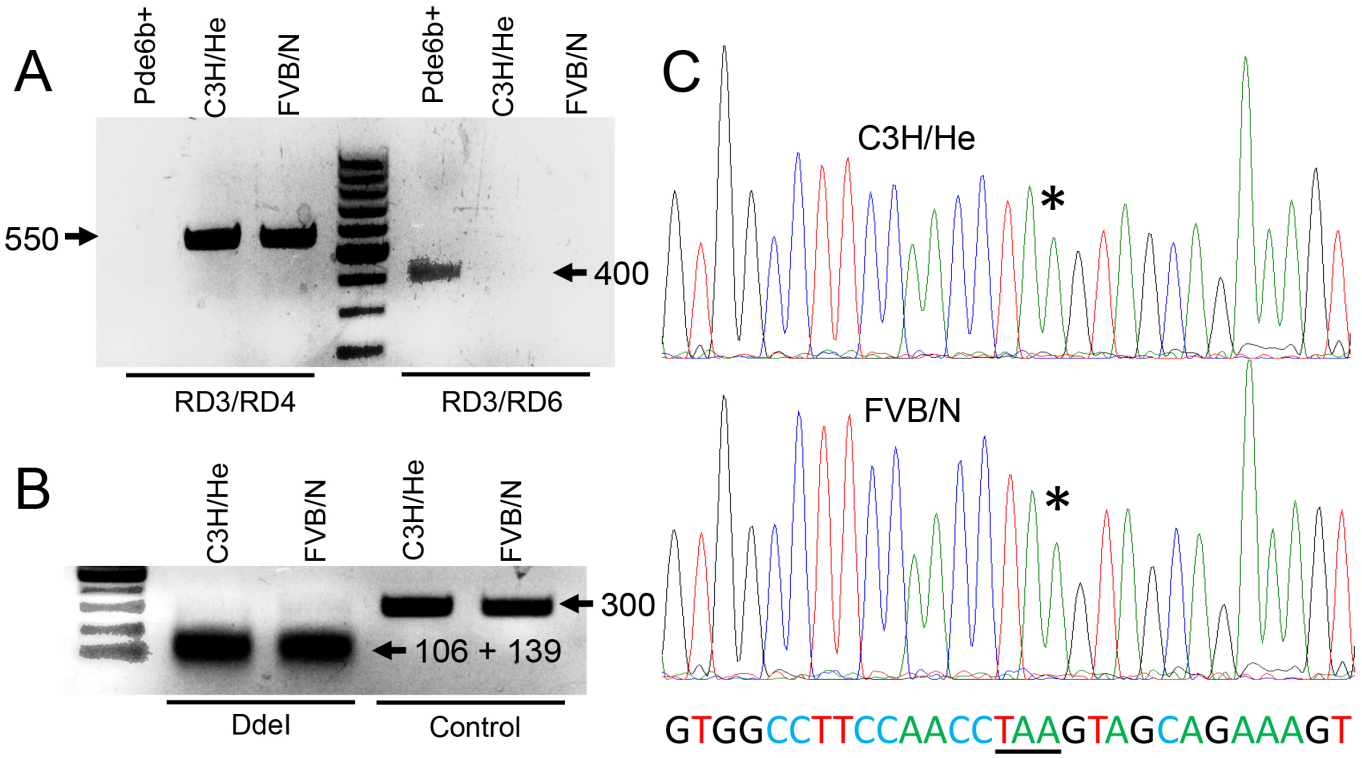

Figure 2. Confirmation of the *rd1* genotype of FVB/N and C3H/HeOu mice. **A**: Presence of the provirus insertion in intron 1 of the *PDE6B* gene tested with Giménez and Montoliu's three-primer method [54]. The primer pair RD3/RD4 amplifies a 550 bp product only in *rd1* lines, whereas the primer pair RD3/RD6 amplifies a 400 bp product only in Pde6b$^+$ control mice. **B**: The nonsense mutation in codon 347 of *rd1* creates a DdeI restriction site. Digestion of a 300 bp PCR product spanning the mutation site with DdeI yielded two diagnostic fragments of 106 bp and 139 bp in both *rd1* strains. Control: uncut 300 bp PCR product. **C**: DNA sequencing over Tyr347 (underlined) confirms the C→A mutation (*) introducing a stop codon (TAA) in both *rd1* strains.

The relatively weak—or completely absent—ERG in young *rd1* mice, which still have a high percentage of responding ganglion cells, closely corresponds to clinical observations where reduced ERG traces are recorded long before significant photoreceptor loss or blindness occurs [63].

Optokinetic response: To go beyond the retina, we behaviorally probed for the integrity of the visual reflex circuitry by testing the maximum spatial frequency able to trigger an optokinetic reflex (OKR). Again, the performances of the seeing FVB-Pde6b$^+$ and C3H-Pde6b$^+$ mice were similar with maximum spatial frequencies of 0.359±0.037 cyc/deg and 0.366±0.011 cyc/deg, respectively, corresponding closely to that of C57/BL6 mice [51]. In line with the ERG results, the 4-week-old C3H/HeOu mice responded to the moving grating, but only to the spatial frequency perceived best by mice (0.062±0.026 cyc/deg). The number of C3H/HeOu mice with a tracking reflex steadily declined with age until no mice responded at 24 weeks (Figure 7). Equal to the ERG experiments, we were not able to measure an OKR response at any time point in the FVB/N mice.

In summary, our results suggest delayed photoreceptor degeneration in C3H/HeOu mice compared to FVB/N mice. Since we observed no significant difference in performance between the two seeing Pde6b$^+$ mouse lines, these data indicate variable phenotypic expressivity of the same *rd1* mutation, with significantly faster age-dependent degeneration in the FVB/N mice compared to the C3H/HeOu mice.

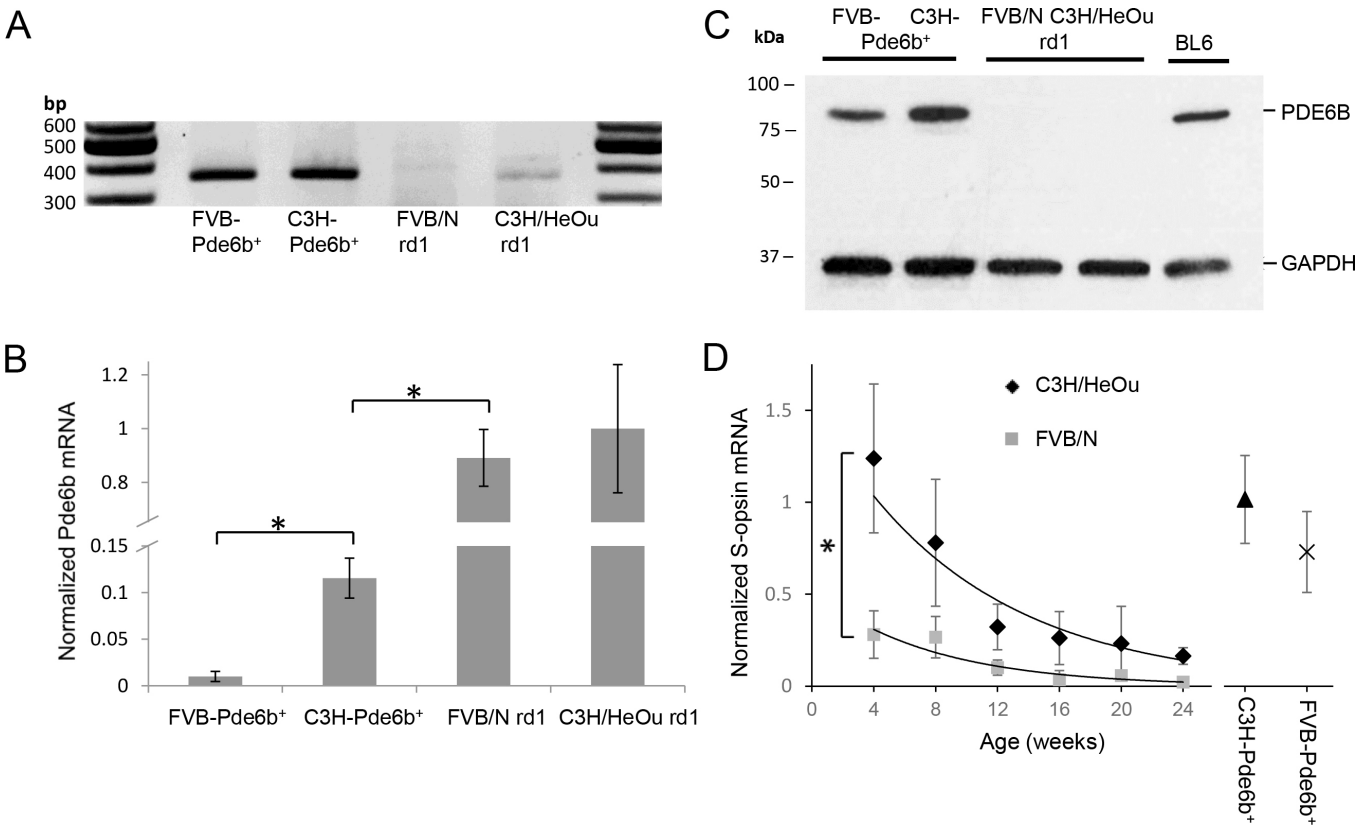

Figure 3. Quantification of Pde6b and S-opsin expression in 3-week old mice. **A**: Agarose gel electrophoresis of the qPCR products with *Pde6b* specific primers. The 359 bp *Pde6b* amplicon is detectable in all four mouse strains, however, at markedly different expression levels. **B**: Normalized Pde6b mRNA levels are significantly higher in C3H/HeOu compared to FVB/N mice, but indistinguishable in the two Pde6b$^+$ control strains. For each group, n=7–8 retinas from four mice. **C**: β-PDE immunoreactivity of retinal protein extracts from Pde6b$^+$, *rd1*, and C57BL/6 wild-type mice at postnatal day 21 using an antibody specific for the N-terminal region of β-PDE. An anti-GAPDH antibody detecting a band of approximately 37 kDa was used as a loading control. No β-PDE expression is detected in *rd1* strains. **D**: Age-dependent S-opsin transcript levels. No significant differences exist between the two Pde6b$^+$ lines and young, 4- to 8-week-old C3H/HeOu mice. In contrast, the S-opsin transcripts in the retinas from 4-week-old FVB/N mice were significantly lower than in coeval C3H/HeOu retinas. For each group, n=6 retinas from three mice. Error bars indicate standard deviation (SD). The fits are exponential with the R-square values for C3H/HeOu and FVB/N at 0.92 and 0.87, respectively.

DISCUSSION

Clinical severity and disease phenotype often differ among individuals with the same genetic mutation, mostly as a result of secondary genetic factors [64]. In RP, such variable phenotypic expressivity is most noticeable in families in whom some affected individuals develop serious visual impairments in early childhood while others live decades with the same primary mutation going unnoticed [15]. Despite the known importance of secondary genetic traits in hereditary photoreceptor degeneration of humans [64] and mice [65,66], variable phenotypic expressivity in the *rd1* mouse model has never been directly addressed. In this study, we emphasize the importance of phenotypic expressivity in *rd1* mice by describing marked differences in the progression of retinal degeneration caused by an identical Pde6b^{rd1} mutation in two common *rd1* strains, C3H/HeOu and FVB/N.

Since the cone photoreceptors are last to degenerate in *rd1* mice and therefore determine the ultimate time point of retinal blindness, we focused on cone degeneration and accordingly conducted OKR, patch-clamp, and ERG recordings at photopic light intensities and targeted immunocytochemistry and qPCR experiments to cone opsin. All methods show a marked difference between the FVB/N and C3H/HeOu mice, with relatively fast degeneration in FVB/N compared to C3H/HeOu mice. Congenic Pde6b^{+} variants of both mouse lines had normal vision with no inherent differences that could account for the differences observed in the *rd1* lines. Sequencing of the *Pde6b* gene in the FVB/N and C3H/HeOu mice confirmed that both strains were *rd1*, suggesting that differences in the progression of degeneration must arise from secondary genetic traits. In other words, modifier genes associated with the C3H/HeOu and FVB/N genetic backgrounds most probably determine the time point and severity of retinal degeneration [64].

Overall, our observed timeline of retinal degeneration in C3H/HeOu mice lies somewhere between the published data

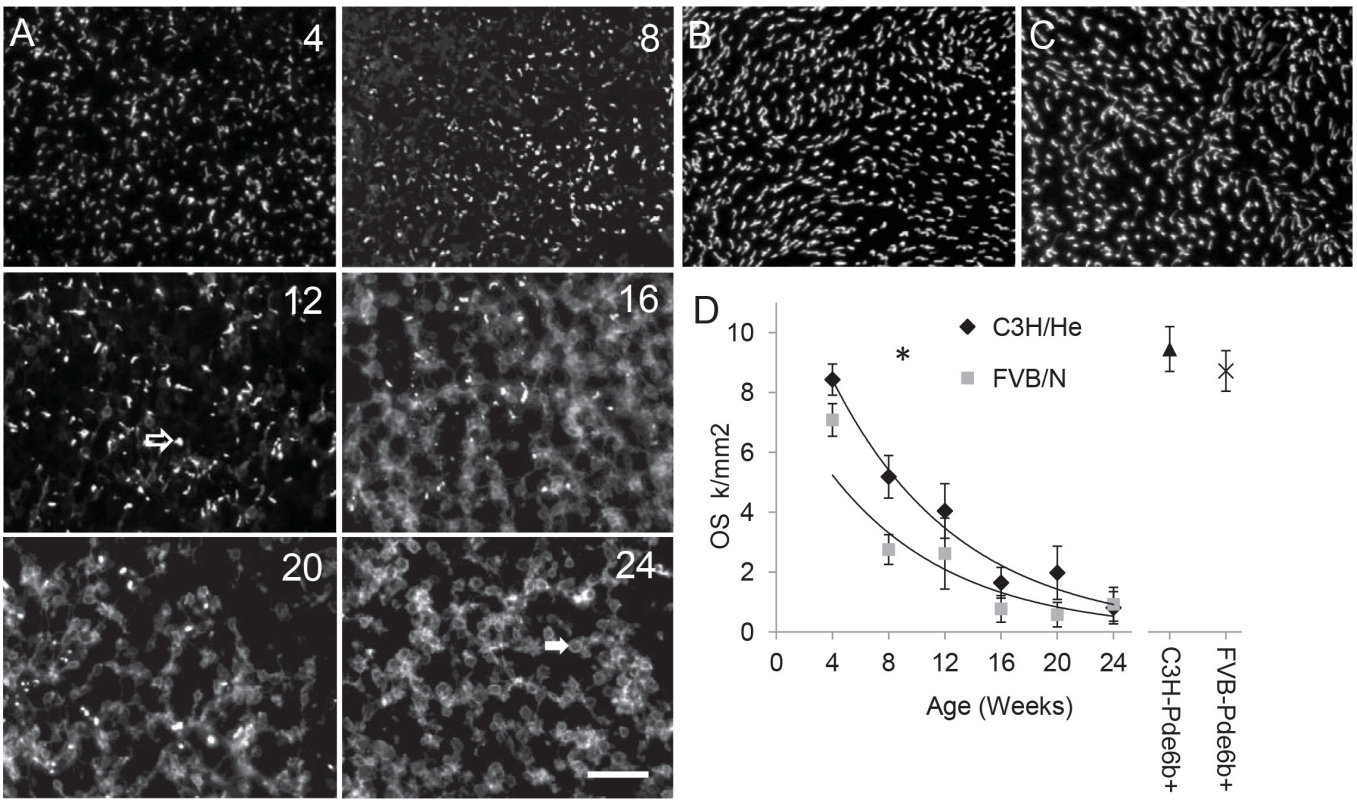

Figure 4. Immunocytochemical detection of cone opsin. Images were always taken from the retinal area with the highest density of labeled cones, typically in the mid-periphery of the retina. **A**: Examples of S-opsin staining in C3H/HeOu retinas demonstrate the progressive loss of cone outer segments and a concomitant accumulation of S-opsin in the cell bodies. One misshaped outer segment (*clear arrow*) and one soma without outer segments (OS) are indicated (*solid arrow*). Age, in weeks, is indicated in the top right of every panel. Scale bar=50 µm. **B**, **C**: S-opsin staining in wild-type C3H-Pde6b^{+} (**B**) and FVB-Pde6b^{+} (**C**) retinas were similar. **D**: Summary graph of OS counts in *rd1* C3H/HeOu and FVB/N mice relative to the Pde6b^{+} mouse lines. For each group, n=8 retinas from four mice. The fits are exponential with the R-square values for C3H/HeOu and FVB/N at 0.94 and 0.8, respectively.

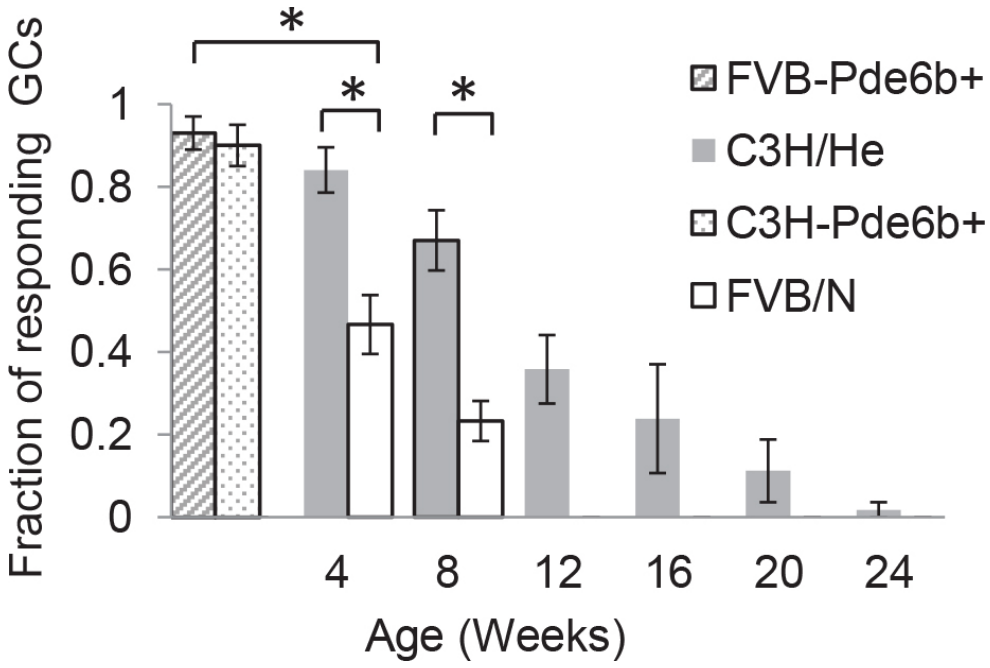

Figure 5. Fraction of retinal ganglion cells responding to a light step in isolated retinas. In both seeing Pde6b$^+$ mouse lines, over 90% of the retinal ganglion cells (GCs) responded to light, with no significant difference between the C3H/He-Pde6b$^+$ and FVB/N-Pde6b$^+$ lines. At 4 weeks, the fraction of responding GCs in the C3H/HeOu mice approximated that of Pde6b$^+$ mice, while the number of responding cells in the age-matched FVB/N mice was already significantly reduced. No responding GCs remained in the FVB/N mice at 12 weeks of age compared to the C3H/HeOu mice where retinal responsiveness disappeared only at 24 weeks of age. For each group, n=6 retinas from six different mice.

for *rd1* and *rd10* mice (Pde6b^{rd10}), an alternative RP mouse model with a missense mutation in exon 13 of the *Pde6b* gene and delayed onset as well as slower progression of retinal degeneration [4,56], while the timeline of degeneration is typical *rd1* in FVB/N mice. In the C3H/HeOu mice, primary rod degeneration and secondary cone OS loss were delayed and only nearly complete at 24 weeks. The same trend was observed in our physiological experiments. Although by postnatal week 12 the FVB/N mice had lost all retinal light responses, ganglion cells from the C3H/HeOu retinas continued to respond until postnatal week 24. Although the 4-week-old FVB/N mice had no ERG, ERG was still detected in the 4-week-old C3H/HeOu mice. For comparison, previous literature report a complete loss of the *rd1* ERG by PND21 [18,23] but ERG responses up to 8 weeks of age in *rd10* mice [23,56,67,68].

Although the morphological phenotype of C3H mice has been stable in the literature over the course of at least 40 years [69], if not 90 years [7], the loss of the C3H ERG by P21 must be treated with caution since the discovery of a spontaneous no b-wave (*nob5*) mutation in C3H/He lines. This mutation in the "parental" C3H/HeJ line was first unmasked when it was crossed to a congenic C3H line lacking the Pde6b mutation [42,70], as the retinal degeneration concealed the *nob5* phenotype. The *nob5* mutation lies in the *Gpr179* gene encoding a protein important for ON-bipolar cell activity by setting the state of the TRPM1 output channels [70,71]. Lack of ON-bipolar cell activity leads to the absence of the b-wave in ERG recordings, even under photopic activation where cones still generate an a-wave [23]. Since the "parental" C3H/HeJ line and some of its substrains are known to carry the *nob5* mutation [72,73], we performed PCR using previously published primers [74] and confirmed that our four mouse lines are negative for *nob5*. However, since functional studies on *rd1* mice are almost non-exclusively performed with ERG, we would like to warn researchers using C3H strains about drawing premature conclusions about non-functional vision as this could be a consequence of the *nob5* and not the *rd1* phenotype.

In line with our electrophysiological results, we still recorded OKR responses in 4-week-old C3H/HeOu mice, while no OKR responses were elicited in the FVB/N mice. Since the ganglion cells in the FVB/N mice still responded to light at postnatal week 8, we do not attribute the lack of ERG and OKR responses to total peripheral blindness but to weak retinal output and possibly underdeveloped or deteriorated central pathways. This is supported by previous work suggesting that rod death precedes full retinal development in *rd1* mice, which compromises the formation of activity-dependent cortical pathways [75,76]. In contrast, degeneration in *rd10* mice starts after full retinal development [68]. Stronger output from young C3H/HeOu retinas may therefore

potentially lead to better development or better preservation of visual pathways compared to the coeval FVB/N mice.

One potentially important difference between the four mouse lines we used is that the FVB/N mice, as opposed to the C3H/HeOu and seeing strains, are albinos. Multiple studies have reported relatively poor vision in albinos [51,77]. This has been partly attributed to the lack of melanin, which naturally reduces the amount of light entering and scattering within the eye, thus protecting the retina against photodamage at high light intensities [78-80]. As the mice were housed at light intensities (approximately 7 lux) shown to be "safe" for albino mice [50], the photodamage in the FVB/N mice in this study is minimal. Other vision problems attributed to albinism, but not directly to light damage, include a reduction in the number of photoreceptor cells, a relative increase in the amount of ganglion cells and miswiring of axons in the optic chiasm [81-85]. Since different albino strains suffer from different degrees of visual impairment, it is hard to judge whether these effects are due to albinism itself. Wong and Brown (2006) [86] conducted a comprehensive study, which compared visual acuity between 14 mouse strains and showed that visual acuity was not directly related to albinism but stems from other genetic traits. For example, the causative locus for poor vision in BALB/c mice is separate from that for albinism [86,87]. In addition, expression of retinal degeneration is unaffected by albinism [88]. Therefore, although a contribution by albinism cannot be absolutely excluded, we conclude that albinism itself is unlikely to underlie the relatively fast retinal degeneration we observed in the FVB/N mice.

The retinas of the 3-week-old FVB/N mice suffered a more advanced pathology compared to the coeval C3H/HeOu retinas. Despite being present at similar numbers, the cone OS had more atypical morphologies compared to the C3H/HeOu mice. In addition, S-opsin and Pde6b mRNA was markedly reduced in the FVB/N retinas. Since β-PDE

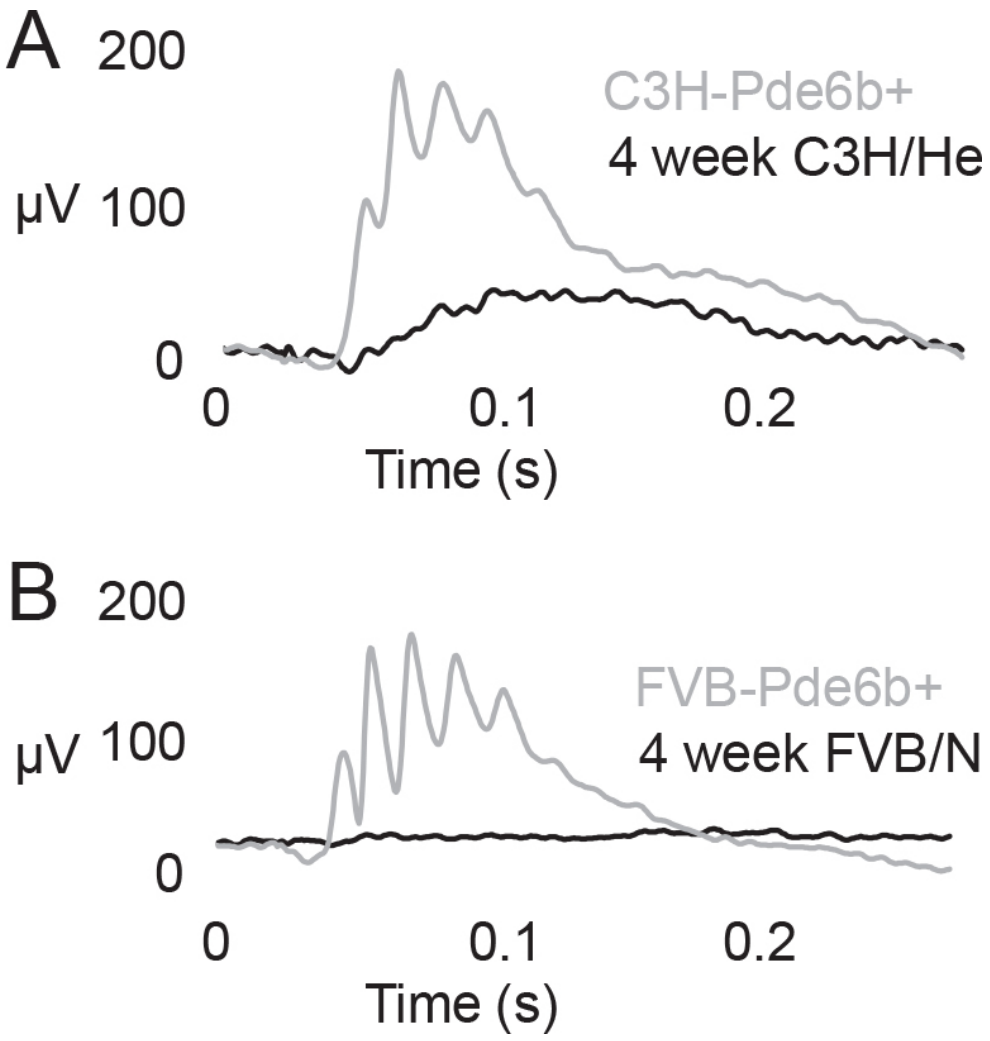

Figure 6. Photopic flash electroretinogram (ERG) recordings. In both Pde6b^{+} mouse lines, we recorded strong responses, with no significant difference in amplitudes. In contrast, the ERGs recorded from the 4-week-old C3H/HeOu mice were markedly weaker with a delayed b-wave that disappeared in older mice. No ERG response was recorded in the FVB/N mice at any time point. For each group, n=6 mice.

is specific to rod photoreceptors [55,89], the reduced Pde6b mRNA levels in FVB/N suggest a more advanced rod loss. This is morphologically apparent from the thin ONL (one-row thick) observed in 3-week-old FVB/N mice. Therefore, the different rates of cone OS degeneration in the two *rd1* strains may be a secondary effect, which reflects relative differences in the speed of rod degeneration.

The potential reasons for the decreased Pde6b mRNA levels in the FVB/N retinas are manifold, and we can only speculate. Aberrant splicing of preRNA and specific degradation of mutant Pde6b mRNA transcripts have been reported to reduce mRNA levels in *rd1* mice [55,90]. In theory, such mechanisms could also account for the differences in the Pde6b mRNA levels of FVB/N and C3H/HeOu retinas if they manifested to different degrees in the two lines. However, *Pde6b* transcription itself could vary in the two *rd1* lines. Although *Pde6b* mRNA was detected, no β-PDE protein was detectably expressed in any of the two *rd1* retinas. This finding is in line with previous reports on *rd1* [56] and could be the consequence of nonsense-mediated Pde6b mRNA decay [55], upregulation of specific micro-RNAs mediating Pde6b translation block, or cotranslational β-PDE modifications such as known myristoylation-reducing protein activity and stability. Although the β-PDE protein was detected in *rd10* retinas [56] and not in *rd1* retinas, marginal expression of the truncated β-PDE protein cannot be exclusively ruled out. Such truncated protein may exhibit some function as it retains the inhibitory γ-subunit-binding site and the cGMP binding domains. Therefore, the observed differences in photoreceptor degeneration in the FVB/N and C3H/HeOu mice could speculatively still arise from differences in β-PDE protein activity or stability. Additional *Pde6b* mutations can modify β-PDE activity and *rd1* phenotype. For example, the chemically induced H620Q missense mutation located in the β-PDE catalytic domain was reported to lead to a slower onset of retinal degeneration in heterozygous Pde6b$^{H620Q/rd1}$ mice compared to homozygous *rd1* mice [9]. Similarly, the artificially introduced homozygous H258N missense mutation in the cGMP-binding domain of β-PDE led to photoreceptor rescue in *rd1* mice [91]. Interestingly, the degree of rescue depended on the genetic background. Mutations in other genomic loci than the *Pde6b* gene itself can therefore

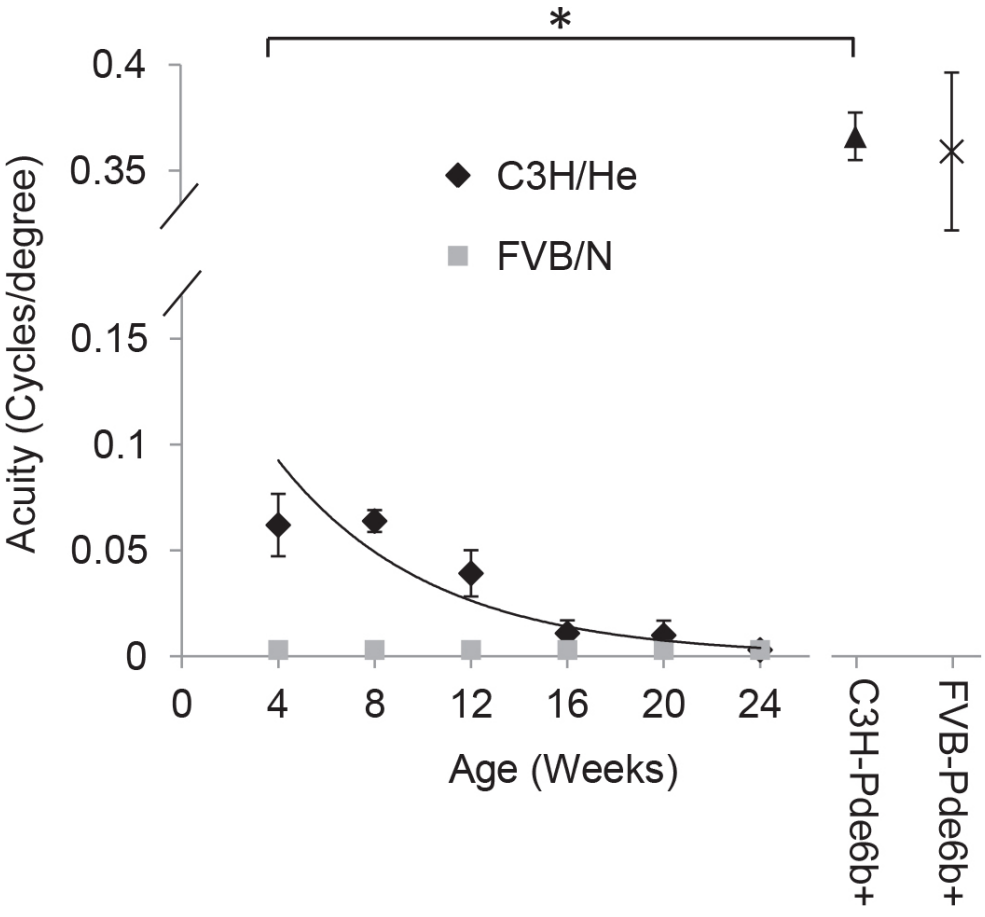

Figure 7. Maximum spatial acuity of the optokinetic reflex (OKR) responses. Although both Pde6b^{+} mouse lines responded to spatial frequencies characteristic of wild-type mice with no significant difference between the two mouse lines, only young 4-week-old C3H/HeOu mice reliably responded with a tracking reflex and only to relatively low spatial frequencies (0.062±0.02 cyc/deg). The number of C3H/HeOu mice with an OKR response decreased steadily with age and approached zero at 24 weeks. The FVB/N mice did not have a detectable OKR at any age. The fit is exponential with an R-square value of 0.92.

potentially influence the *rd1* phenotype. For example, a point mutation in the mitochondrial *mt-ATP8* gene [46] of FVB/N mice was attributed to increased oxidative stress [47,48], which could, at least in part, contribute to accelerated photoreceptor death. Alternatively, the cone OS in the C3H/HeOu mice might be better preserved by an unknown mechanism. It has recently been shown that miR-182 and miR-183 foster cone OS maintenance [92]. Different levels of miRNAs in the two *rd1* strains could consequently underlie different rates of OS degeneration. Since the modifier genes responsible for the different phenotypes observed in FVB/N and C3H/HeOu mice may lie in any genomic region, it might be necessary to identify trait loci and candidate genes as the next step toward identifying genes associated with phenotypic expressivity in *rd1* mice [93].

Since retinal degeneration in FVB/N mice overlaps with retinal development and FVB/N mice may also have relatively underdeveloped central visual pathways, they may be a less useful RP model for vision recovery studies compared to C3H/HeOu mice. In light of the results presented in this study, we assume similar variable phenotypic expressivity between *rd10* mouse lines. Since *rd10* mice equally have a mutation in the *Pde6b* gene, degeneration is likely to be much slower on the C3H/HeOu background compared to the FVB/N background. In conclusion, our results highlight the important role of genetic background in the *rd1* pathology promoting a more accurate comparison and interpretation of results collected from different *rd* mouse lines. To avoid variation resulting from differences in genetic background altogether, it may be sensible to use only one *rd1* mouse line in preclinical studies. Additionally, our results move toward identifying and understanding secondary genetic traits that govern variable phenotypic expressivity in patients with RP.

ACKNOWLEDGMENTS

We thank Maria Misteli for her help with the OKR and immunocytochemistry experiments, Myriam Siffert for breeding the mice, Volker Enzmann for providing the OKR setup and Jasmin Balmer and Ange Maguy for technical assistance. This work was supported by grants from the Swiss National Science Foundation (31003A_152807/1), the Haag-Streit Holding AG; and the Commission for Technology and Innovation (CTI, N° 14,341.1 PFLS-LS).

REFERENCES

1. Busskamp V, Roska B. Optogenetic approaches to restoring visual function in retinitis pigmentosa. Curr Opin Neurobiol 2011; 21:942-6. [PMID: 21708457].
2. Cronin T, Vandenberghe L, Hantz P, Juttner J, Reimann A, Kacsó A, Huckfeldt R, Busskamp V, Kohler H, Lagali P, Roska B, Bennett J. Efficient transduction and optogenetic stimulation of retinal bipolar cells by a synthetic adeno-associated virus capsid and promoter. EMBO Mol Med 2014; 6:1175-90. [PMID: 25092770].
3. Caporale N, Kolstad K, Lee T, Tochitsky I, Dalkara D, Trauner D, Kramer R, Dan Y, Isacoff E, Flannery J. LiGluR restores visual responses in rodent models of inherited blindness. Mol Ther 2011; 19:1219-29. [PMID: 21610698].
4. Chang B, Hawes NL, Hurd RE, Davisson MT, Nusinowitz S, Heckenlively JR. Retinal degeneration mutants in the mouse. Vision Res 2002; 42:517-25. [PMID: 11853768].
5. Bowes C, Li T, Frankel WN, Danciger M, Coffin JM, Applebury ML, Farber DB. Localization of a retroviral element within the rd gene coding for the beta subunit of cGMP phosphodiesterase. Proc Natl Acad Sci USA 1993; 90:2955-9. [PMID: 8385352].
6. Pittler SJ, Baehr W. Identification of a nonsense mutation in the rod photoreceptor cGMP phosphodiesterase beta-subunit gene of the rd mouse. Proc Natl Acad Sci USA 1991; 88:8322-6. [PMID: 1656438].
7. Keeler CE. The Inheritance of a Retinal Abnormality in White Mice. Proc Natl Acad Sci USA 1924; 10:329-33. [PMID: 16576828].
8. McLaughlin ME, Ehrhart T, Berson E, Dryja T. Mutation spectrum of the gene encoding the beta subunit of rod phosphodiesterase among patients with autosomal recessive retinitis pigmentosa. Proc Natl Acad Sci USA 1995; 92:3249-53. [PMID: 7724547].
9. Davis RJ, Tosi J, Janisch KM, Kasanuki JM, Wang NK, Kong J, Tsui I, Cilluffo M, Woodruff ML, Fain GL, Lin CS, Tsang SH. Functional rescue of degenerating photoreceptors in mice homozygous for a hypomorphic cGMP phosphodiesterase 6 b allele (Pde6bH620Q). Invest Ophthalmol Vis Sci 2008; 49:5067-76. [PMID: 18658088].
10. Hartong DT, Berson EL, Dryja TP. Retinitis pigmentosa. Lancet 2006; 368:1795-809. [PMID: 17113430].
11. Shintani K, Shechtman D, Gurwood A. Review and update: current treatment trends for patients with retinitis pigmentosa. Optometry 2009; 80:384-401. [PMID: 19545852].
12. Thyagarajan S, van Wyk M, Lehmann K, Lowel S, Feng G, Wassle H. Visual function in mice with photoreceptor degeneration and transgenic expression of channelrhodopsin 2 in ganglion cells. J Neurosci 2010; 30:8745-58. [PMID: 20592196].
13. Jay M, Bird AC, Moore AN, Jay B. Nine generations of a family with autosomal dominant retinitis pigmentosa and evidence of variable expressivity from census records. J Med Genet 1992; 29:906-10. [PMID: 1479605].
14. Jelcick AS, Yuan Y, Leehy BD, Cox LC, Silveira AC, Qiu F, Schenk S, Sachs AJ, Morrison MA, Nystuen AM, DeAngelis MM, Haider NB. Genetic variations strongly influence

phenotypic outcome in the mouse retina. PLoS ONE 2011; 6:e21858-[PMID: 21779340].

15. Vaclavik V, Gaillard MC, Tiab L, Schorderet DF, Munier FL. Variable phenotypic expressivity in a Swiss family with autosomal dominant retinitis pigmentosa due to a T494M mutation in the PRPF3 gene. Mol Vis 2010; 16:467-75. [PMID: 20309403].
16. Stasheff SF, Shankar M, Andrews MP. Developmental time course distinguishes changes in spontaneous and light-evoked retinal ganglion cell activity in rd1 and rd10 mice. J Neurophysiol 2011; 105:3002-9. [PMID: 21389300].
17. Carter-Dawson LD, LaVail M, Sidman R. Differential effect of the rd mutation on rods and cones in the mouse retina. Invest Ophthalmol Vis Sci 1978; 17:489-98. [PMID: 659071].
18. Farber DB, Flannery JG, Bowes-Rickman C. The rd mouse story: seventy years of research on an animal model of inherited retinal degeneration. Prog Retin Eye Res 1994; 13:31-64. .
19. Barabas P, Culter Peck C, Krizaj D. Do calcium channel blockers rescue dying photoreceptors in the *Pde6b*^{rd1} mouse? Adv Exp Med Biol 2010; 664:491-9. [PMID: 20238051].
20. Hart AW, McKie L, Morgan J, Cautier P, West K, Jackson I, Cross S. Genotype-phenotype correlation of mouse Pde6b mutations. Invest Ophthalmol Vis Sci 2005; 46:3443-50. [PMID: 16123450].
21. Farber DB, Lolley RN. Cyclic guanosine monophosphate: elevation in degenerating photoreceptor cells of the C3H mouse retina. Science 1974; 186:449-51. [PMID: 4369896].
22. Farber DB, Lolley RN. Enzymic basis for cyclic GMP accumulation in degenerative photoreceptor cells of mouse retina. J Cyclic Nucleotide Res 1976; 2:139-48. [PMID: 6493].
23. Gibson R, Fletcher E, Vingrys A, Zhu Y, Vessey K, Kalloniatis M. Functional and neurochemical development in the normal and degenerating mouse retina. J Comp Neurol 2013; 521:1251-67. [PMID: 23238927].
24. Grubb SC, Maddatu TP, Bult CJ, Bogue MA. Mouse phenome database. Nucleic Acids Res 2009; 37:720-30. .
25. LaVail MM, Sidman RL. C57BL-6J mice with inherited retinal degeneration. Arch Ophthalmol 1974; 91:394-400. [PMID: 4595403].
26. Chang B, Hurd R, Wang J, Nishina P. Survey of common eye diseases in laboratory mouse strains. Invest Ophthalmol Vis Sci 2013; 54:4974-81. [PMID: 23800770].
27. Nishiguchi KM, Carvalho L. Rizz iM, Powell K, Holthaus S, Azam S, Duran Y, Ribeiro J, Luhmann U, Bainbridge J, Smith A, Ali R. Gene therapy restores vision in rd1 mice after removal of a confounding mutation in Gpr179. Nat Commun 2015; 6:6006-21. [PMID: 25613321].
28. Lagali PS, Balya D, Awatramani GB, Munch TA, Kim DS, Busskamp V, Cepko CL, Roska B. Light-activated channels targeted to ON bipolar cells restore visual function in retinal degeneration. Nat Neurosci 2008; 11:667-75. [PMID: 18432197].
29. Lin B, Koizumi A, Tanaka N, Panda S, Masland RH. Restoration of visual function in retinal degeneration mice by ectopic expression of melanopsin. Proc Natl Acad Sci USA 2008; 105:16009-14. [PMID: 18836071].
30. Canola K, Angenieux B, Tekaya M, Quiambao A, Naash MI, Munier FL, Schorderet DF, Arsenijevic Y. Retinal stem cells transplanted into models of late stages of retinitis pigmentosa preferentially adopt a glial or a retinal ganglion cell fate. Invest Ophthalmol Vis Sci 2007; 48:446-54. [PMID: 17197566].
31. Li T, Adamian M, Roof DJ, Berson EL, Dryja TP, Roessler BJ, Davidson BL. In vivo transfer of a reporter gene to the retina mediated by an adenoviral vector. Invest Ophthalmol Vis Sci 1994; 35:2543-9. [PMID: 8163343].
32. Li T, Lewallen M, Chen S, Yu W, Zhang N, Xie T. Multipotent stem cells isolated from the adult mouse retina are capable of producing functional photoreceptor cells. Cell Res 2013; 23:788-802. [PMID: 23567557].
33. Roesch K, Stadler MB, Cepko CL. Gene expression changes within Muller glial cells in retinitis pigmentosa. Mol Vis 2012; 18:1197-214. [PMID: 22665967].
34. Auerbach AB, Norinsky R, Ho W, Losos K, Guo Q, Chatterjee S, Joyner AL. Strain-dependent differences in the efficiency of transgenic mouse production. Transgenic Res 2003; 12:59-69. [PMID: 12650525].
35. Taketo M, Schroeder A, Mobraaten L, Gunning K, Hanten G, Fox R, Roderick T, Stewart C, Lilly F, Hansen C. FVB/N: an inbred mouse strain preferable for transgenic analyses. Proc Natl Acad Sci USA 1991; 88:2065-9. [PMID: 1848692].
36. Hoelter SM, Dalke C, Kallnik M, Becker L, Horsch M, Schrewe A, Favor J, Klopstock T, Beckers J, Ivandic B, Gailus-Durner V, Fuchs H, Hrabé de Angelis M, Graw J. W W. "Sighted C3H" mice–a tool for analysing the influence of vision on mouse behaviour? Front Biosci 2008; 13:5810-23. [PMID: 18508624].
37. Errijgers V, Van Dam D, Gantois I, Van Ginneken CJ, Grossman AW, D'Hooge R, De Deyn PP, Kooy RF. FVB.129P2-Pde6b(+) Tyr(c-ch)/Ant, a sighted variant of the FVB/N mouse strain suitable for behavioral analysis. Genes Brain Behav 2007; 6:552-7. [PMID: 17083330].
38. ES R. Hereditary anemias of the mouse: a review for geneticists. Adv Genet 1979; 20:357-459. [PMID: 390999].
39. Poltorak A, He X, Smirnova I, Liu M, Van Huffel C, Du X, Birdwell D, Alejos E, Silva M, Galanos C, Freudenberg M, Ricciardi-Castagnoli P, Layton B, Beutler B. Defective LPS signaling in C3H/HeJ and C57BL/10ScCr mice: mutations in Tlr4 gene. Science 1998; 282:2085-8. [PMID: 9851930].
40. Tokuda S, Beyer B, Frankel W. Genetic complexity of absence seizures in substrains of C3H mice. Genes Brain Behav 2009; 8:283-9. [PMID: 19170754].
41. Frankel W, Mahaffey C, McGarr T, Beyeler B, Letts V. Unravelling genetic modifiers in the gria4 mouse model of absence epilepsy. PLoS Genet 2014; 10:e1004454-.

42. Ray T. Constructing the rod bipolar cell signalplex using animal models of retinal dysfunction. 2014.

43. Pan H, Yan B-S, Rojas M, Shebzukhov Y, Zhou H, Kobzik L, Higgins D, Daly M, Bloom B, Kramnik I. Ipr1 gene mediates innate immunity to tuberculosis. Nature 2005; 434:767-72. [PMID: 15815631].

44. Ritchie DJ, Clapcote S. Disc1 deletion is present in Swiss-derived inbred mouse strains: implications for transgenic studies of learning and memory. Lab Anim 2013; 47:162-7. [PMID: 23563120].

45. Bauer K, Yu X, Wernhoff P, Koczan D, Thiesen H, Ibrahim S. Identification of new quantitative trait loci in mice with collagen-induced arthritis. Arthritis Rheum 2004; 50:3721-8. [PMID: 15529344].

46. Yu X, Wester-Rosenlöf L, Gimsa U, Holzhueter S, Marques A, Jonas L, Hagenow K, Kunz M, Nizze H, Tiedge M, Holmdahl R, Ibrahim S. The mtDNA nt7778 G/T polymorphism affects autoimmune diseases and reproductive performance in the mouse. Hum Mol Genet 2009; 18:4689-98. [PMID: 19759059].

47. Weiss H, Wester-Rosenlöf L, Koch C, Baltrusch S, Tiedge M, Ibrahim S. The mitochondrial Atp8 mutation induces mitochondrial ROS generation, secretory dysfunction, and β-cell mass adaptation in conplastic B6-mtFVB mice. Endocrinology 2012; 153:4666-76. [PMID: 22919063].

48. Eipel C, Hildebrandt A, Scholz B, Schyschka L, Minor T, Kreikemeyer B, Ibrahim S, Vollmar B. Mutation of mitochondrial ATP8 gene improves hepatic energy status in a murine model of acute endotoxemic liver failure. Life Sci 2011; 88:343-9. [PMID: 21167184].

49. Errijgers V, Van Dam D, Gantois I, Van Ginneken C, Grossman A, D'Hooge R, De Deyn P, Kooy R. FVB.129P2-Pde6b+ Tyrc-ch/Ant, a sighted variant of the FVB/N mouse strain suitable for behavioural analysis. Genes Brain Behav 2007; 6:552-7. [PMID: 17083330].

50. Institute for Laboratory Animal Research; Division on Earth and Life Studies. Guide for the care and use of laboratory animals. The National Academic Press. 2011

51. Prusky GT, Alam NM, Beekman S, Douglas RM. Rapid quantification of adult and developing mouse spatial vision using a virtual optomotor system. Invest Ophthalmol Vis Sci 2004; 45:4611-6. [PMID: 15557474].

52. Zulliger R, Lecaude S, Eigeldinger-Berthou S, Wolf-Schnurrbusch UE, Enzmann V. Caspase-3-independent photoreceptor degeneration by N-methyl-N-nitrosourea (MNU) induces morphological and functional changes in the mouse retina. Graefes Arch Clin Exp Ophthalmol 2011; 249:859-69. [PMID: 21240523].

53. Schneider CA, Rasband WS, Eliceiri KW. NIH Image to ImageJ: 25 years of image analysis. Nat Methods 2012; 9:671-5. [PMID: 22930834].

54. Giménez E, Montoliu L. A simple polymerase chain reaction assay for genotyping the retinal degeneration mutation (Pde6brd) in FVB/N-derived transgenic mice. Lab Anim 2001; 35:153-6. [PMID: 11315164].

55. Yan W, Lewin A, Hauswirth W. Selective degradation of nonsense beta-phosphodiesterase mRNA in the heterozygous rd mouse. Invest Ophthalmol Vis Sci 1998; 39:2529-36. [PMID: 9856762].

56. Chang B, Hawes N, Pardue M, German A, Hurd R, Davisson M, Nusinowitz S, Rengarajan K, Boyd A, Sidney S, Phillips M, Stewart R, Chaudhury R, Nickerson J, Heckenlively J, Boatright J. Two mouse retinal degenerations caused by missense mutations in the beta-subunit of rod cGMP phosphodiesterase gene. Vision Res 2007; 47:624-33. [PMID: 17267005].

57. Zhang X, Cote R. cGMP signaling in vertebrate retinal photoreceptor cells. Front Biosci 2005; 10:1191-204. [PMID: 15769618].

58. Lin B, Masland R, Strettoi E. Remodeling of cone photoreceptor cells after rod degeneration in rd mice. Exp Eye Res 2009; 88:589-99. [PMID: 19087876].

59. Applebury MM, Antoch M, Baxter L, Chun L, Falk J, Farhangfar F, Kage K, Krzystolik M, Lyass L, Robbins J. The murine cone photoreceptor: a single cone type expresses both S and M opsins with retinal spatial patterning. Neuron 2000; 27:513-23. [PMID: 11055434].

60. Bowes C, Li T, Danciger M, Baxter L, Applebury M, Farber D. Retinal degeneration in the rd mouse is caused by a defect in the beta subunit of rod cGMP-phosphodiesterase. Nature 1990; 347:677-80. [PMID: 1977087].

61. Cleland BG, Levick WR. Properties of rarely encountered types of ganglion cells in the cat's retina and an overall classification. J Physiol 1974; 240:457-92. [PMID: 4420300].

62. Berson DM, Dunn FA, Takao M. Phototransduction by retinal ganglion cells that set the circadian clock. Science 2002; 295:1070-3. [PMID: 11834835].

63. Tsang S, Wolpert K. The Genetics of Retinitis Pigmentosa. Retinal Physician 2010

64. Nadeau JH. Modifier genes in mice and humans. Nat Rev Genet 2001; 2:165-74. [PMID: 11256068].

65. Humphries MM, Kiang S, McNally N, Donovan M, Sieving P, Bush R, Machida SC. T, Hobson A, Farrar J, Humphries P, Kenna P. Comparative structural and functional analysis of photoreceptor neurons of Rho−/− mice reveal increased survival on C57BL/6J in comparison to 129Sv genetic background. Vis Neurosci 2001; 18:437-43. [PMID: 11497420].

66. Matsumoto H, Kataoka K, Tsoka P, Connor K, Miller J, Vavvas D. Strain difference in photoreceptor cell death after retinal detachment in mice. Invest Ophthalmol Vis Sci 2014; 55:4165-74. [PMID: 24854853].

67. Pang JJ, Boye S, Kumar A, Dinculescu A, Deng W, Li J, Li Q, Rani A, Foster T, Chang B, Hawes N, Boatright J, Hauswirth W. AAV-Mediated Gene Therapy for Retinal Degeneration in the rd10 Mouse Containing a Recessive PDEβ Mutation. Invest Ophthalmol Vis Sci 2008; 49:4278-83. [PMID: 18586879].

68. Gargini C, Terzibasi E, Mazzoni F, Strettoi E. Retinal organization in the retinal degeneration 10 (rd10) mutatnt mouse: a morhphological and ERG study. J Comp Neurol 2007; 500:222-38. [PMID: 17111372].

69. Sanyal S, Bal A. Comparative light and electron microscopic study of retinal histogenesis in normal and rd mutant mice. Z Anat Entwicklungsgesch 1973; 142:219-38. [PMID: 4781863].

70. Peachey NS, Ray T, Florijn R, Rowe L, Sjoerdsma T, Contreras-Alcantara S, Baba K, Tosini G, Pozdeyev N, Iuvone P, Bojang PJ, Pearring J, Simonsz H, van Genderen M, Birch D. Traboulsi iE, Dorfman A, Lopez I, Ren H, Goldberg A, Nishina P, Lachapelle F, McCall M, Koenekoop R, Bergen A, Kamermans M, RG G. GPR179 is required for depolarizing bipolar cell function and is mutated in autosomal-recessive complete congenital stationary night blindness. Am J Hum Genet 2012; 90:331-9. [PMID: 22325362].

71. Ray TA, Heath K, Hasan N, Noel J, Samuels I, Martemyanov K, Peachey N, McCall M. RG G. GPR179 is required for high sensitivity of the mGluR6 signaling cascade in depolarizing bipolar cells. J Neurosci 2014; 34:6334-43. [PMID: 24790204].

72. Nishiguchi KM, Carvalho L, Rizzi M, Powell K, Holthaus S, Azam S, Duran Y, Ribeiro J, Luhmann U, Bainbridge J, Smith A, Ali R. Gene therapy restores vision in rd1 mice after removal of a confounding mutation in Gpr179. Nat Commun 2015; 6:6006-21. [PMID: 25613321].

73. Peachey NS, Ray T, Florijn R, Rowe L, Sjoerdsma T, Contreras-Alcantara S, Baba K, Tosini G, Pozdeyev N, Iuvone P, Bojang P, Pearring J, Simonsz H, van Genderen M, Birch D, Traboulsi E, Dorfman A, Lopez I, Ren H, Goldberg A, Nishina P, Lachapelle F, McCall M, Koenekoop R, Bergen A, Kamermans M, Gregg R. GPR179 is required for depolarizing bipolar cell function and is mutated in autosomal-recessive complete congenital stationary night blindness. Am J Hum Genet 2012; 90:331-9. [PMID: 22325362].

74. Balmer J, Ji R, Ray T, Selber F, Gassmann M, Peachey N, Gregg R, Enzmann V. Presence of the Gpr179(nob5) allele in a C3H-derived transgenic mouse. Mol Vis 2013; 19:2615-25. [PMID: 24415894].

75. Chua J, Fletcher EL, Kalloniatis M. Functional remodeling of glutamate receptors by inner retinal neurons occurs from an early stage of retinal degeneration. J Comp Neurol 2009; 514:473-91. [PMID: 19350664].

76. Wong RO. Retinal waves and visual system development. Annu Rev Neurosci 1999; 22:29-47. [PMID: 10202531].

77. Creel DJ, Dustman RE, Beck EC. Differences in visually evoked responses in albino versus hooded rats. Exp Neurol 1970; 29:298-309. [PMID: 5504472].

78. Greenman DL, Bryant P, Kodell RL, Sheldon W. Influence of cage shelf level on retinal atrophy in mice. Lab Anim Sci 1982; 32:353-6. [PMID: 7144107].

79. LaVail MM, Gorrin GM, Repaci MA. Strain differences in sensitivity to light-induced photoreceptor degeneration in albino mice. Curr Eye Res 1987; 6:825-34. [PMID: 3608569].

80. Hayes JM, Balkema G. Visual thresholds in mice: comparison of retinal light damage and hypopigmentation. Vis Neurosci 1993; 10:931-8. [PMID: 8217942].

81. Creel D, Witkop CJ Jr, King RA. Asymmetric visually evoked potentials in human albinos: evidence for visual system anomalies. Invest Ophthalmol 1974; 13:430-40. [PMID: 4831697].

82. Fulton AB, Albert DM, Craft JL. Human albinism. Light and electron microscopy study. Arch Ophthalmol 1978; 96:305-10. [PMID: 629678].

83. Grant S, Patel NN, Philp AR, Grey CN, Lucas RD, Foster RG, Bowmaker JK, Jeffery G. Rod photopigment deficits in albinos are specific to mammals and arise during retinal development. Vis Neurosci 2001; 18:245-51. [PMID: 11417799].

84. Guillery RW, Okoro AN, Witkop CJ Jr. Abnormal visual pathways in the brain of a human albino. Brain Res 1975; 96:373-7. [PMID: 1175020].

85. Rachel RA, Dolen G, Hayes NL, Lu A, Erskine L, Nowakowski RS, Mason CA. Spatiotemporal features of early neuronogenesis differ in wild-type and albino mouse retina. J Neurosci 2002; 22:4249-63. [PMID: 12040030].

86. Wong AA, Brown RE. Visual detection, pattern discrimination and visual acuity in 14 strains of mice. Genes Brain Behav 2006; 5:389-403. [PMID: 16879633].

87. Puk O, Dalke C, Hrabe de Angelis M, Graw J. Variation of the response to the optokinetic drum among various strains of mice. Front Biosci 2008; 13:6269-75. [PMID: 18508659].

88. Ward R. Quantitative effects of retinal degeneration in mice. Rev Can Biol Exp 1982; 41:115-9. [PMID: 6890226].

89. Viczian A, Sanyal S, Toffenetti J, Chader G, Farber D. Photoreceptor-specific mRNAs in mice carrying different allelic combinations at the rd and rds loci. Exp Eye Res 1992; 54:853-60. [PMID: 1381682].

90. Muradov H, Boyd K, Kerov V, Artemyev N. Atypical retinal degeneration 3 in mice is caused by defective PDE6B pre-mRNA splicing. Vision Res 2012; 57:1-8. [PMID: 22326271].

91. Tsang SH, Woodruff M, Jun L, Mahajan V, Yamashita C, Pedersen R, Lin C, Goff S, Rosenberg T, Larsen M, Farber D, Nusinowitz S. Transgenic mice carrying the H258N mutation in the gene encoding the beta-subunit of phosphodiesterase-6 (PDE6B) provide a model for human congenital stationary night blindness. Hum Mutat 2007; 28:243-54. [PMID: 17044014].

92. Busskamp V, Krol J, Nelidova D, Daum J, Szikra T, Tsuda B, Jüttner J, Farrow K, Scherf B, Alvarez C, Genoud C, Sothilingam V, Tanimoto N, Stadler M, Seeliger M, Stoffel M, Filipowicz W. B R. miRNAs 182 and 183 are necessary to maintain adult cone photoreceptor outer segments and visual function. Neuron 2014; 83:586-600. [PMID: 25002228].

93. Danciger M, Ogando D, Yang H, Matthes M, Yu N, Ahern K, Yasumura D, Williams R, Lavail M. Genetic modifiers of retinal degeneration in the rd3 mouse. Invest Ophthalmol Vis Sci 2008; 49:2863-9. [PMID: 18344445].

Articles are provided courtesy of Emory University and the Zhongshan Ophthalmic Center, Sun Yat-sen University, P.R. China. The print version of this article was created on 31 July 2015. This reflects all typographical corrections and errata to the article through that date. Details of any changes may be found in the online version of the article.